

Sequence-based bioinformatic prediction and QUASEP identify genomic imprinting of the *KCNK9* potassium channel gene in mouse and human

Nico Ruf^{1,2}, Sylvia Bähring³, Danuta Galetzka⁴, Galyna Pliushch⁴, Friedrich C. Luft³, Peter Nürnberg⁵, Thomas Haaf⁴, Gavin Kelsey² and Ulrich Zechner^{4,*}

¹Max-Delbrueck-Center for Molecular Medicine, D-13125 Berlin, Germany, ²Laboratory of Developmental Genetics and Imprinting, The Babraham Institute, Cambridge CB22 3AT, UK, ³Franz Volhard Clinic, Charité, University Medical School, D-13122 Berlin, Germany, ⁴Institute of Human Genetics, Johannes Gutenberg University Mainz, Langenbeckstraße 1, D-55131 Mainz, Germany and ⁵Cologne Center for Genomics and Institute for Genetics, University of Cologne, D-50674 Cologne, Germany

Received June 12, 2007; Revised July 19, 2007; Accepted July 30, 2007

Genomic imprinting is the epigenetic marking of gene subsets resulting in monoallelic or predominant expression of one of the two parental alleles according to their parental origin. We describe the systematic experimental verification of a prioritized 16 candidate imprinted gene set predicted by sequence-based bioinformatic analyses. We used Quantification of Allele-Specific Expression by Pyrosequencing (QUASEP) and discovered maternal-specific imprinted expression of the *Kcnk9* gene as well as strain-dependent preferential expression of the *Rarres1* gene in E11.5 (C57BL/6 × Cast/Ei)F1 and informative (C57BL/6 × Cast/Ei) × C57BL/6 backcross mouse embryos. For the remaining 14 candidate imprinted genes, we observed biallelic expression. In adult mouse tissues, we found that *Kcnk9* expression was restricted to the brain and also was maternal-specific. QUASEP analysis of informative human fetal brain samples further demonstrated maternal-specific imprinted expression of the human *KCNK9* orthologue. The CpG islands associated with the mouse and human *Kcnk9/KCNK9* genes were not differentially methylated, but strongly hypomethylated. Thus, we speculate that mouse *Kcnk9* imprinting may be regulated by the maternal germline differentially methylated region in *Peg13*, an imprinted non-coding RNA gene in close proximity to *Kcnk9* on distal mouse chromosome 15. Our data have major implications for the proposed role of *Kcnk9* in neurodevelopment, apoptosis and tumorigenesis, as well as for the efficiency of sequence-based bioinformatic predictions of novel imprinted genes.

INTRODUCTION

Imprinted genes are exclusively or predominantly expressed from only one of their two parental alleles (1). The imprints are parent-specific epigenetic modifications of DNA and chromatin that are erased and established when the gene passes through the germline (2). Aberrant genomic imprinting can cause human diseases, including disorders affecting

development and behaviour. Loss of imprinting (LOI) is often associated with human cancers. Increasing evidence also supports a role for imprinted genes in the pathogenesis of obesity, diabetes and malformations after assisted reproductive technology and mammalian embryo cloning (3). To date, more than 80 imprinted transcripts are known in mice and humans (4). Imprinted genes frequently cluster in domains with imprinting control centres that are shared by

*To whom correspondence should be addressed. Tel: +49 6131175850; Fax: +49 6131175689; Email: zechner@humgen.klinik.uni-mainz.de

multiple neighbouring imprinted genes. However, several examples of imprinted genes occurring apparently isolated in the mouse and human genomes have also been described (5,6).

Most approaches to identify novel imprinted genes have determined differential expression of maternal and paternal alleles by subtractive hybridization, differential mRNA display or cDNA microarray screening (5,6). Recently, Luedi *et al.* (7) described an innovative bioinformatics approach, in which specific DNA sequence characteristics of known imprinted genes were used to screen for novel potentially imprinted genes. In a first step, they analysed 44 known imprinted genes for the presence and position of specific sequence motifs such as repetitive elements, transcription factor binding sites and CpG islands. Subsequently, Luedi *et al.* used the collected data to train a classifier for the prediction of either imprinted or non-imprinted expression and the parental allele preferentially expressed. Application of this classifier to a total of 23 788 mouse genes resulted in the prediction of 600 candidate imprinted genes, 64% of which were predicted to be maternally expressed. These candidate imprinted genes provide an excellent resource for the identification of causative genes in multifactorial diseases associated with parent-of-origin differences.

In an earlier study, we described the successful application of Quantification of Allele-Specific Expression by Pyrosequencing (QUASEP) for experimental validation of candidate imprinted genes selected from an expression profiling study of uniparental mouse embryos (8,9). We identified three novel imprinted transcripts encoding putative non-protein-coding RNAs on the basis of parent-of-origin-specific monoallelic expression in E11.5 (C57BL/6 × Cast/Ei)F1 and informative (C57BL/6 × Cast/Ei) × C57BL/6 backcross embryos. In addition, we found four transcripts with preferential expression of a strain-specific allele.

In the present study, we also used QUASEP to experimentally validate a prioritized set of 16 promising candidate imprinted genes selected from the bioinformatics prediction of Luedi *et al.* (7). We identified one novel imprinted gene, *Kcnk9*, which is already known to play an important role in apoptosis and tumorigenesis as well as neuronal development and function.

RESULTS

Selection of promising candidate genes

We extracted 600 murine candidate imprinted genes and their prediction strength from the previous bioinformatics study (7). On the basis of prediction strength, associated biomedical interest as well as properties shared with known imprinted genes (e.g. proximity to other candidate genes and, thus, potential clustered organization), we subsequently selected 18 promising candidate imprinted genes for experimental validation (Table 1, Supplementary Material, Table S1).

Identification of tSNPs and QUASEP analysis

For imprinting analysis, we used the previously described QUASEP method (9,10). This method, based on Pyrosequencing™ technology, enables the discrimination of subtle differences in

allele-specific transcript ratios and uses heterozygous transcribed single nucleotide polymorphisms (tSNPs) for distinguishing the parental origin of a transcribed allele. Thus, we screened the selected 18 candidate imprinted genes for tSNPs by sequencing genomic DNA samples derived from C57BL/6, Cast/Ei and interspecific (C57BL/6 × Cast/Ei)F1 hybrid mice. Using the Pyrosequencing Assay Design software, we identified tSNPs appropriate for QUASEP in 16 of these genes (Supplementary Material, Table S2). Then, we evaluated the imprinted expression of these 16 candidate imprinted genes by QUASEP of RT-PCR products derived from (C57BL/6 × Cast/Ei)F1, C57BL/6 and Cast/Ei E11.5 whole embryos.

We identified monoallelic expression of the maternal allele of *Kcnk9* predicted by Luedi *et al.* (7). Furthermore and in contrast to the bioinformatics prediction, we observed preferential expression of the paternal allele of *Rarres1*. The remaining 14 candidate imprinted genes showed biallelic expression (Table 1). To confirm the putative imprinted expression of *Kcnk9* and *Rarres1*, we performed a QUASEP analysis of informative embryos derived from reciprocal (C57BL/6 × Cast/Ei) × C57BL/6 crosses. In these experiments, the *Kcnk9* gene again exhibited monoallelic expression of the predicted maternal allele, confirming imprinting (Fig. 1A, Supplementary Material, Fig. S1A), whereas the preferential expression of *Rarres1* turned out to be strain-specific and not imprinted (data not shown). We further confirmed imprinted expression of *Kcnk9* by conventional sequence analysis of the tSNP in the corresponding RT-PCR product (Supplementary Material, Fig. S2).

Maintenance of imprinted *Kcnk9* expression in the adult stage

To address whether imprinted expression of *Kcnk9* is also maintained in the adult, we performed RT-PCR to determine *Kcnk9* expression in skeletal muscle, kidney, liver, lung, heart, brain, testis and spleen. *Kcnk9* RT-PCR products were detected only in adult brain, but not in the other tissues (Fig. 2). QUASEP assays with RT-PCR products from adult brain of (C57BL/6 × Cast/Ei)F1 as well as informative reciprocal backcross mice revealed complete maintenance of monoallelic maternal *Kcnk9* expression in adult brain (Fig. 1B, Supplementary Material, Fig. S1B).

Imprinted expression of the human *KCNK9* orthologue

Many genes that are imprinted in the mouse are also imprinted in humans (1,4). Therefore, we analysed the allele-specific expression of the human *KCNK9* gene, which is predominantly expressed in brain (11,12). We tested 15 fetal brain DNA samples by genomic PCR and conventional sequence analysis and found that seven were heterozygous for the known T/C-SNP in exon 2 of *KCNK9* (NCBI dbSNP: rs2615374). We further performed QUASEP assays with RT-PCR products from the seven heterozygous samples (T/C) and detected strict or predominant monoallelic expression from either the T- or the C-allele (Fig. 1C, Supplementary Material, Fig. S1C). As the maternal deciduas for two heterozygous samples expressing the T-allele and C-allele, respectively,

Table 1. Allelic expression analysis of the studied candidate imprinted genes

Gene	Ensembl-ID (<i>Mus musculus</i>)	Expression predicted	Chromosome including cytogenetic band and coordinate (in base pairs)	Allelic expression ratio (C57BL/6J: Cast/Ei)
<i>Kcnk9</i>	ENSMUSG00000036760	Maternal	15e3 (72591862–72626022)	Monoallelic maternal (99%: 1%; SD 1.6)
<i>Hes5</i>	ENSMUSG00000048001	Paternal	4e2 (153950465–153951913)	No expressed SNP available
<i>Nkx6-2</i>	ENSMUSG000000041309	Maternal	7f5 (135993086–135996580)	Biallelic (43%: 57%; SD 2.2)
<i>Ntng2</i>	ENSMUSG000000035513	Maternal	2a3 (29202132–29255351)	Biallelic (51%: 49%; SD 3.2)
<i>Camk2b</i>	ENSMUSG000000020466	Paternal	11a1 (5921675–6017751)	Biallelic (51%: 49%; SD 3.9)
<i>Irx4</i>	ENSMUSG000000021604	Maternal	13c1 (70192290–70201087)	Biallelic (50%: 50%; SD 1.6)
<i>Rarres1</i>	ENSMUSG000000049404	Maternal	3e2 (67579972–67616619)	Preferential strain-specific Cast/Ei (33%: 67%; SD 9.3)
<i>Foxg1</i>	ENSMUSG000000020950	Paternal	12c1 (47396718–47400567)	Biallelic (49%: 51%; SD 0.6)
<i>Dok1</i>	ENSMUSG00000000694	Paternal	6d1 (83056368–83058899)	Biallelic (54%: 46%; SD 1.8)
<i>Wnt7b</i>	ENSMUSG000000022382	Maternal	15e3 (85617762–85663903)	Biallelic (53%: 47%; SD 3.4)
<i>Disc1</i>	ENSMUSG000000043051	Paternal	8e2 (123641593–123849582)	No expressed SNP available
<i>Ly6d</i>	ENSMUSG000000034634	Maternal	15e1 (74842606–74844117)	Biallelic (59%: 41%; SD 4.2)
<i>Gdnf</i>	ENSMUSG000000022144	Maternal	15a2 (7637824–7664388)	Biallelic (47%: 53%; SD 2.4)
<i>Cdk6</i>	ENSMUSG000000033820	Maternal	5a1 (3350318–3528231)	Biallelic (47%: 53%; SD 1.4)
<i>Gad2</i>	ENSMUSG000000026787	Maternal	2a3 (22607267–22675939)	Biallelic (50%: 50%; SD 1.5)
<i>Nppc</i>	ENSMUSG000000026241	Maternal	1c5 (86566967–86571248)	Biallelic (55%: 45%; SD 2.8)
<i>Prdm16</i>	ENSMUSG000000039410	Paternal	4e2 (153309834–153626302)	Biallelic (52%: 48%; SD 0.9)
<i>Stk32c</i>	ENSMUSG000000015981	Maternal	7f5 (135523291–135602224)	Biallelic (52%: 48%. SD 4.1)

SD, standard deviation (calculated from at least four samples); genes are sorted by descending prediction strengths.

were homozygous for the T (T/T) and C alleles (C/C), respectively (data not shown), we concluded that the expressed allele was of maternal origin.

Identification and methylation analysis of CpG islands

Many imprinted genes are associated with CpG islands, showing differential methylation of maternal and paternal alleles [termed differentially methylated regions (DMRs)] (1,6,13). Consequently, the proximity of CpG islands was an important feature for the genome-wide prediction of novel imprinted genes by Luedi *et al.* (7). To identify CpG islands associated with the murine *Kcnk9* gene and its human orthologue, we used the EMBOSS CpGPlot tool. The program identified putative CpG islands within the promoter regions of both orthologues, reaching from –1326 to +153 bp in the mouse (denoted mCpG1 in Fig. 3A) and from –1498 to +640 bp in the human (denoted hCpG1 in Fig. 3B), each with respect to the translational start codon. In addition, we detected multiple putative binding sites (mouse: $n = 2$ and human: $n = 6$) of the methylation-sensitive CTCF insulator protein within these CpG-rich regions (14). Thus, we performed bisulphite sequencing of mouse adult brain and spleen genomic DNA samples, as well as human fetal brain and blood DNA samples, to investigate both CpG islands for the presence of differential methylation. This analysis revealed that both mCpG1 and hCpG1 are not differentially methylated, but instead strongly hypomethylated (Fig. 4A and B). Consequently, a mechanism other than DNA methylation of their promoter regions is presumably involved in regulating the imprinted expression of the mouse and human *Kcnk9/KCNK9* genes.

In the mouse, *Kcnk9* is located on chromosome 15 ~260 kb downstream of the imprinted *Peg13* gene, a non-protein-coding RNA gene of unknown function (Fig. 3A). Similar to *Kcnk9*, *Peg13* is expressed predominantly in brain, but, in contrast, the maternal allele is silenced and marked by DNA methylation in somatic tissues (15). We therefore hypothesized that imprinting of the murine *Kcnk9* gene is controlled by the *Peg13*-DMR (located from +195 to +833 bp relative to the 5' end of the *Peg13* transcript and denoted mCpG2 in Fig. 3A). To lend support to this hypothesis, we performed bisulphite sequence analysis of the *Peg13*-DMR in male and female germ cells. We found full methylation of the *Peg13*-DMR in mature oocytes and near complete absence of methylation in sperm DNA (Fig. 4C).

Although there was no direct human orthologue of *Peg13* identified, conceivably, the *Peg13*-DMR is at least positionally conserved and differentially methylated in both species and, consequently, also acts as a regulatory region for human *KCNK9* imprinting. The mouse *Peg13*-DMR is located in intron 16 of the gene 1810044A24Rik (also known as *Nibp* or KIAA1882, Fig. 3A) which was already described to be not imprinted (15). Taking into account an additional exon belonging to the 5'-untranslated region of human *NIBP*, the *Peg13*-DMR orthologous region in humans is located in intron 17 of *NIBP* on chromosome 8q24.3. In this region, the EMBOSS CpGPlot tool identified a 730 bp CpG island (located from –75 316 to –74 586 bp relative to the 5' end of exon 18 of the human *NIBP* gene and denoted hCpG2 in Fig. 3B), with putative CTCF binding sites ($n = 2$). However, bisulphite sequencing of human fetal brain and blood DNA samples showed that hCpG2 is not differentially methylated but strongly hypermethylated (Fig. 4D).

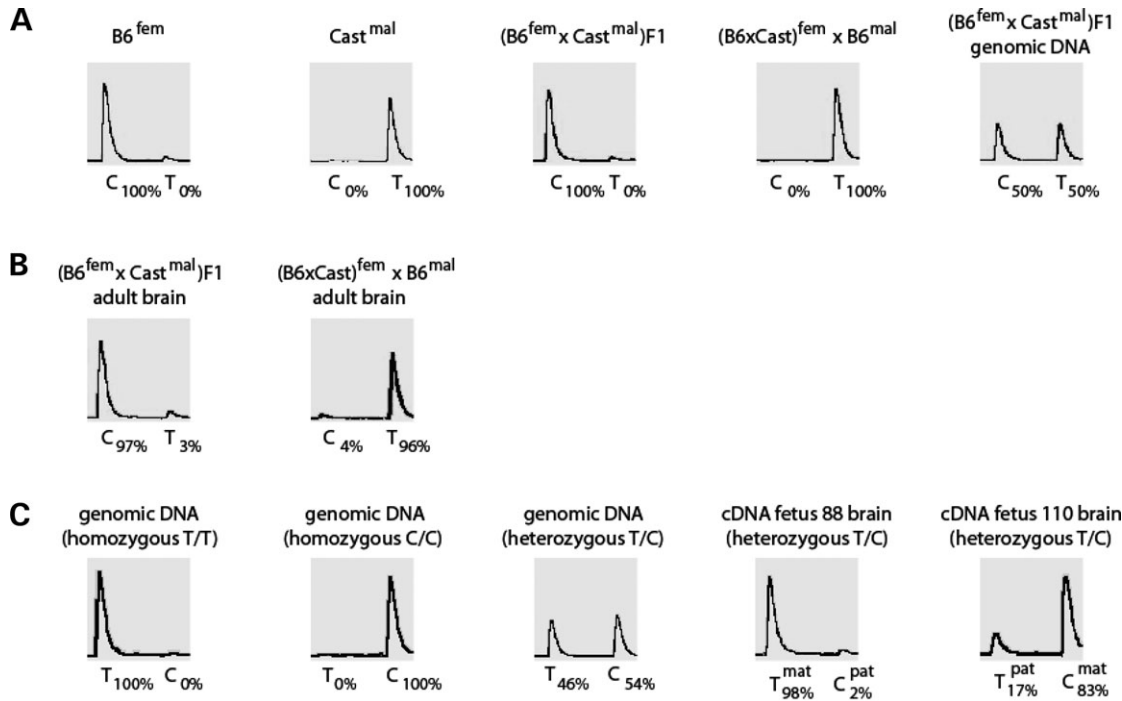


Figure 1. Maternal-specific imprinted expression of the *Kcnk9/KCNK9* genes in mouse and human. (A) Maternal-specific imprinted expression in mouse E11.5 embryos. Four pyrosequencing pyrograms of cDNA derived from C57BL/6, Cast/Ei, (C57BL/6 × Cast/Ei)F1 and informative (C57BL/6 × Cast/Ei) × C57BL/6 E11.5 embryos and one pyrogram of genomic DNA derived from a (C57BL/6 × Cast/Ei)F1 individual are shown. (B) Maintenance of maternal-specific imprinted expression in mouse adult brain. Pyrograms of adult brain cDNA derived from (C57BL/6 × Cast/Ei)F1 and informative (C57BL/6 × Cast/Ei) × C57BL/6 individuals are presented. (C) Maternal-specific imprinted expression of the human *KCNK9* gene in fetal brain. Three pyrograms of genomic DNA derived from two homozygous individuals and one heterozygous individual and two pyrograms of fetal brain cDNAs derived from two heterozygous (T/C) individuals are presented. As the maternal deciduas for these two heterozygous individuals expressing the T-allele (fetus 88) and C-allele (fetus 110), respectively, were homozygous for the T-allele (T/T) (decidua of fetus 88) and C-allele (C/C) (decidua of fetus 110), respectively (data not shown), we concluded that the transcribed allele was of maternal origin. Transcribed SNPs used to discriminate the parental origin of the alleles are given below each pyrogram, together with the percentage of expression obtained after normalization. B6, C57BL/6; Cast, Cast/Ei; fem, female; mal, male; mat, maternally inherited allele; pat, paternally inherited allele.

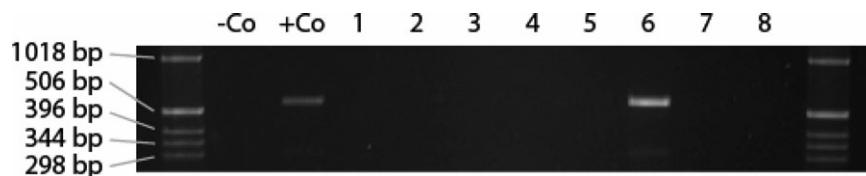


Figure 2. Brain-specific expression of the murine *Kcnk9* gene. RT-PCR assay of the *Kcnk9* transcript indicates amplification from adult brain (lane 6), but not skeletal muscle (lane 1), kidney (lane 2), liver (lane 3), lung (lane 4), heart (lane 5), testis (lane 7) and spleen (lane 8). Lane -Co shows the negative control (blank), whereas lane +Co indicates *Kcnk9* expression in the E11.5 embryo (positive control). The 553 bp RT-PCR product was amplified only from the cDNA template.

DISCUSSION

We used QUASEP of E11.5 (C57BL/6 × Cast/Ei)F1 hybrid embryos to systematically analyse and verify imprinted expression of 16 promising candidate imprinted genes predicted by a recent bioinformatics study. Our analysis identified one novel imprinted gene, *Kcnk9*, and one gene with strain-specific preferential expression, *Rarres1*. The other analysed 14 candidate genes were biallelically expressed. We cannot, however, rule out the possibility that some of the remaining candidates have highly selective, tissue-specific imprinting, which would not have been detected in our analysis.

Kcnk9 belongs to the family of two-pore domain potassium channel genes (K2P) and encodes the TASK-3 protein (16). The K2P channels regulate the resting membrane potential and also influence action potential duration and firing frequency of neurons (16). In humans, TASK-3 is expressed in the brain with particularly high levels in the cerebellum (11). Recent studies indicate a role of TASK-3 in development and maturation of cerebellar neurons (17). In this context, overexpression of TASK-3 has been linked to apoptosis of cerebellar granule neurons (18). The recent description of a *Kcnk9* mutation in a rat model of absence epilepsy further suggests a prominent role of this gene in the central nervous

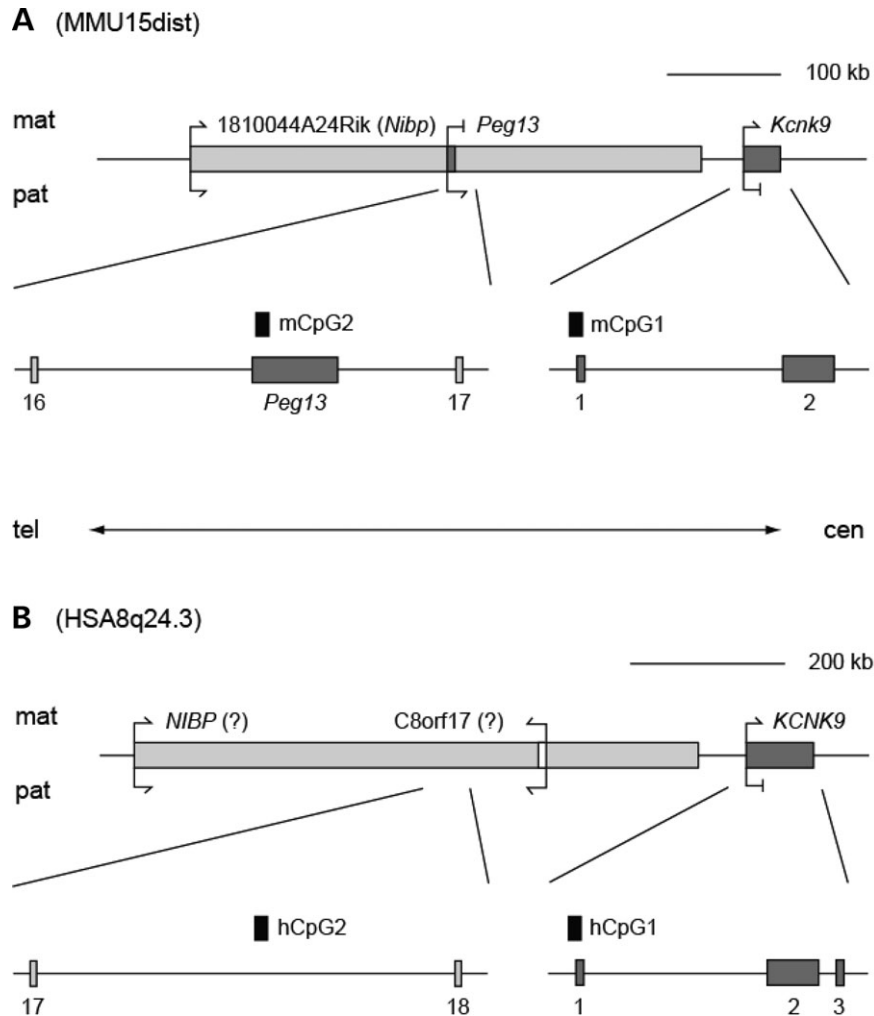


Figure 3. The *Kcnk9*/*KCNK9* and *Nibp*/*NIBP* loci on distal mouse chromosome 15 (A, MMU15dist) and human chromosome 8q24.3 (B, HSA8q24.3), respectively. (A) The murine *Kcnk9* gene together with 1810044A24Rik (also known as *Nibp* and KIAA1882) and *Peg13* are shown. *Kcnk9* and *Peg13* are imprinted genes. 1810044A24Rik was already shown to be not imprinted (15). Each of the enlarged regions harbours a CpG island conserved between mouse and human, mCpG1 and mCpG2: mCpG2 is also known as *Peg13*-DMR and is differentially methylated with methylation of the maternal allele only (15). (B) The human genes *KCNK9*, *NIBP* and *C8orf17* are shown. *KCNK9* is the only imprinted gene identified so far in this region. From data in the mouse, biallelic expression of *NIBP* and *C8orf17* is assumed, but denoted with a question mark. The human 840 kb region is larger than the murine (550 kb), with an additional 5' exon of *NIBP*. No direct human orthologue of *Peg13* is known. The conserved CpG islands are depicted in the enlarged regions (hCpG1 and hCpG2). Imprinted genes are indicated as dark-grey boxes. Biallelically expressed genes are shown as light-grey or white boxes. Arrows indicate the transcriptional status and direction with the maternal allele on top and the paternal allele on bottom. In the enlarged sections, the positions of CpG islands and exons are displayed. Exon numbers are shown below each exon. mat, maternal chromosome; pat, paternal chromosome; tel, telomeric; cen, centromeric.

system (19). Interestingly, aberrant expression of TASK-3 has been repeatedly implicated in tumourigenesis. Mu *et al.* (20) reported that *KCNK9* is amplified from 3- to 10-fold in 10% of breast tumours and overexpressed from 5- to over 100-fold in 44% of breast tumours. Moreover, *KCNK9* was also overexpressed in lung, colon and prostate cancers (20,21). Overexpression of *KCNK9* in cell lines promotes tumour formation and induces resistance to both hypoxia and serum deprivation (20). Furthermore, wild-type *KCNK9* confers a growth advantage to cells, whereas the inactivating mutant has no effect on cell growth, suggesting that *KCNK9* is directly involved in cell proliferation and has oncogenic properties (22).

In this context, the discovery of *Kcnk9* imprinting has important implications. Numerous imprinted genes including

IGF2, *ARH1*, *PEG1/MEST*, *DLK-GTL2* and others have been described to be aberrantly expressed and/or aberrantly methylated in several types of cancers (23). A frequent finding in cancers is LOI, which refers to activation of the normally silenced allele, or silencing of the normally active allele, of an imprinted gene. The best-known example is the LOI of *IGF2*, which is found in both the neighbouring normal cells and the tumour cells in colon, breast and prostate cancers (23). Thus, it is tempting to speculate that the role of *KCNK9* in tumourigenesis and its putative oncogenic properties are not only associated with its overexpression, but also with an LOI.

Both mouse and human *Kcnk9*/*KCNK9* imprinting do not seem to be regulated by short-range *cis*-acting differential methylation at their CpG-island promoter. In this context, it

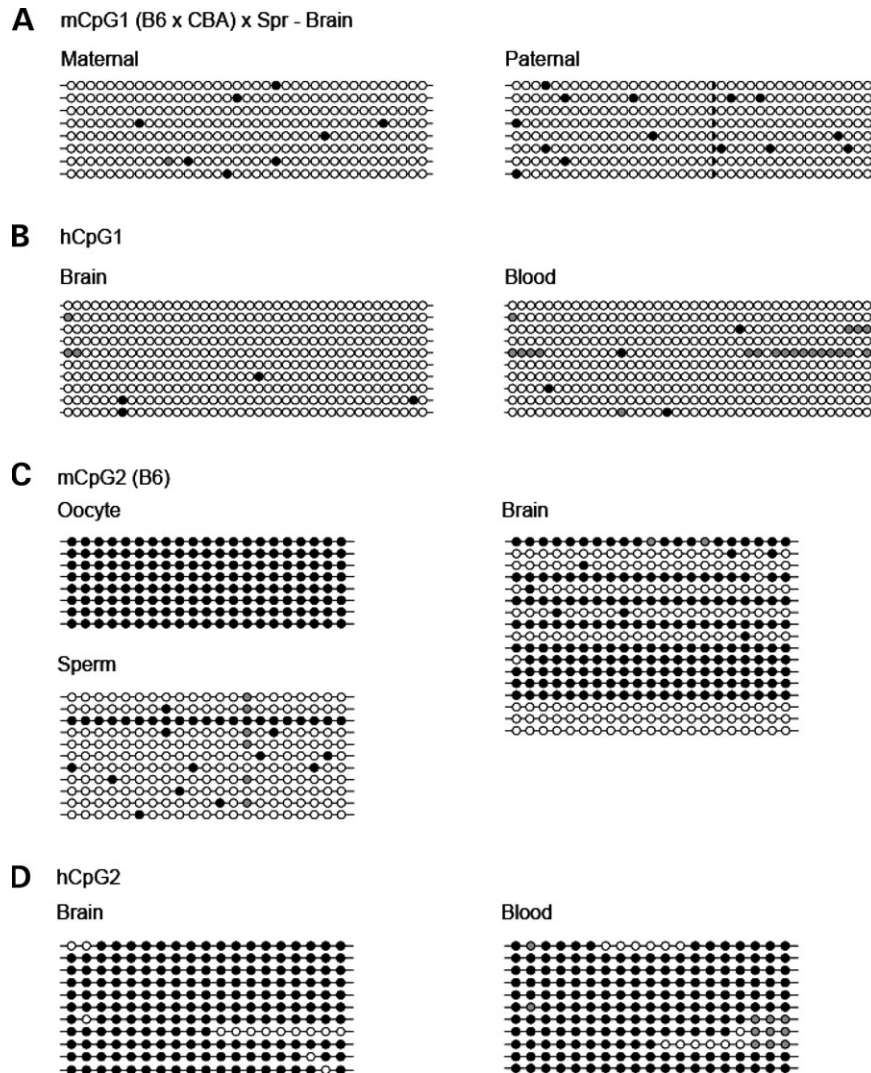


Figure 4. Methylation profiles of CpG islands associated with the murine and human *Kcnk9/KCNK9* genes. The locations of the CpG islands analysed are indicated in Figure 3. Methylation profiles shown derive from sequences of PCR products cloned after amplification of bisulphite-treated DNAs. Unfilled circles represent unmethylated CpGs and filled circles represent methylated CpGs. The shaded circles indicate CpGs whose methylation status could not be determined unequivocally. **(A)** Parental allele-specific methylation profiles of mCpG1 (subregion 1, located from -1365 to -1006 bp relative to the translational start codon of the murine *Kcnk9* gene), maternal and paternal alleles are hypomethylated. The half-filled circles in the paternal alleles indicate a SNP in which a CpG dinucleotide present in B6 (maternal alleles) is modified to a CpA dinucleotide in *M. spretus* (Spr, paternal alleles). **(B)** hCpG1 (located from -668 to -282 bp relative to the translational start codon of the human *KCNK9* gene) methylation profiles demonstrate hypomethylation in human fetal brain and adult blood. **(C)** Methylation profiles of mCpG2 (subregion 1, located from $+166$ to $+463$ bp relative to the 5' end of the murine *Peg13* gene) in B6 oocytes, sperm and brain indicate that this region is a maternal germline DMR. **(D)** Methylation profiles of hCpG2 (located from $-74\,855$ to $-74\,557$ bp relative to the 5' end of exon 18 of the human *NIBP* gene) in human fetal brain and adult blood illustrate hypermethylation of both parental alleles.

can be conjectured that the nearby murine *Peg13*-DMR acts as a long-range acting imprinting control element also capable of controlling the imprinting of the distal murine *Kcnk9* gene, particularly as we have now been able to demonstrate that it is a maternal germline DMR. Intriguingly, however, the *Peg13*-DMR does not appear to confer imprinting on the *Nibp* gene, in an intron of which it resides (15). Several examples of long-range acting imprinting control elements including the *H19*-DMR, the *Lit1*-DMR/*KvDMR1*, the IG-DMR of *Dlk1-Gtl2* and others have already been described in mouse and human (13,24,25). Parent-specific deletion of the *Peg13*-DMR in the mouse followed by parental allele-specific

Kcnk9 expression analysis may reveal a function of the *Peg13*-DMR in murine *Kcnk9* imprinting control. Furthermore, a more detailed analysis of the known expressed sequence tags and associated regulatory regions located in the equivalent intron of human *NIBP* to that which contains *Peg13* in the mouse may lead to the identification of a functional equivalent of *Peg13* and its DMR in humans (15).

In our study, we also identified one gene, *Rarres1*, with a strain-dependent allele-specific transcript bias. *Rarres1* is a retinoid-regulated gene and resides on mouse chromosome 3. Expression of its human orthologue, *RARRES1*, is frequently downregulated through DNA hypermethylation in

several types of cancers (26). Strain-dependent allele-specific transcript biases in the mouse have already been described for several genes (9,27). For four genes, Cowles *et al.* also identified promoter-associated SNPs in the strains analysed, which may act as *cis*-acting regulatory factors and, thus, cause the allele-specific transcript bias. Sequencing of the *Rarres1* promoter in C57BL/6 and Cast/Ei strains may also reveal such candidate regulatory SNPs. With regard to the role of *RARRES1* during tumourigenesis, it will be of interest to determine whether an allele-specific transcript bias of this gene is also found in humans.

Our findings must also be discussed with regard to the efficiency of sequence-based bioinformatics prediction of candidate imprinted genes. In several studies, specific sequence characteristics of imprinted genes have been reported and suggested to be appropriate for distinguishing between mono-allelically and biallelically expressed genes in a genome-wide screen to identify candidate imprinted genes (28–31). Luedi *et al.* (7) performed the first large-scale prediction of imprinted genes on the basis of the DNA sequence characteristics alone. From 600 murine genes predicted to be potentially imprinted, we prioritized 18 promising candidates using different parameters including prediction strength, associated biomedical interest as well as properties shared with known imprinted genes (Table 1, Supplementary Material, Table S1). We could experimentally analyse 16 of 18 genes by QUASEP and identified one gene (6%), *Kcnk9*, to be indeed imprinted. Interestingly, *Kcnk9* was also the most promising candidate of the 18 prioritized genes, as it displayed the highest scores with regard to prediction strength and, thus, the highest priority (Table 1). This finding underscores the strength of the underlying bioinformatics prediction. If one considers that estimates of the total number of imprinted genes in the human and/or mouse genome range from 100 to 200 (3), one would assume an a priori likelihood of imprinting of a gene randomly chosen from the genome of <1%. Thus, the 6% rate of detection of an imprinted gene in our study is at least a six times improvement over chance and evidence for efficiency of the bioinformatics prediction. It is likely that new informatics analyses, for example, the identification of sequence properties correlated with the propensity of CpG islands to be methylated, (32), may further help refine sequence-based imprinted gene predictions.

In summary, our data have major implications for current and future studies analysing the role of *Kcnk9* in neurodevelopment, neurobehaviour, apoptosis and tumourigenesis. In addition, our findings will also strongly influence current and future bioinformatic screens aimed at the identification of novel imprinted genes.

MATERIALS AND METHODS

Mouse and human material

We purchased C57BL/6 (B6) and *Mus musculus castaneus* (Cast/Ei) mice from Charles River Laboratories (Wilmington, MA, USA). We used these mice and their F1 hybrids and reciprocal backcross mice as sources of genomic DNA and total RNA. We performed natural matings to generate timed embryos with the day after conception considered as day

0.5. Note that for F1 hybrid and BC1 progeny, the maternal parent is designated first. For bisulphite sequence analysis of the mouse *Kcnk9* CpG island, DNA was prepared from F1(C57BL/6 × CBA/Ca) × *M. spretus* adult brain; sperm and oocytes DNAs for analysis of the *Peg13*-DMR were obtained from C57BL/6, as described previously (33). For parental allele-specific expression analysis in human, we obtained fetal brain samples from aborted fetuses and matched paraffin-embedded maternal deciduas that underwent pathological examination and cytogenetic analysis in the Department of Paediatric Pathology at Mainz University School of Medicine as sources of genomic DNA and total RNA. The local Ethics Committee [Ärztchamber Rheinland-Pfalz, decision no. 837.103.04 (4261)] approved the use of anonymized ‘excess’ tissue material for scientific analyses. We selected only fetuses without detectable abnormal development and with normal karyotype. We dissected fetal tissues within 24 h after abortion and stored them at –80°C until further analysis.

Isolation of nucleic acids and cDNA synthesis

We prepared genomic DNA using standard salting out procedures or a specialized protocol (for paraffin-embedded deciduas) of the QIAamp DNA Mini Kit (Qiagen, Hilden, Germany). For the preparation of total RNA, we used Trizol reagent (Invitrogen GmbH, Karlsruhe, Germany). Afterwards, all isolated RNA samples were treated with the DNA-free kit (Ambion Ltd, Huntington, UK) to exclude or minimize contamination with genomic DNA. The cDNA samples were subsequently synthesized from 5 µg of each total RNA using an oligo(dT)₁₈ primer and the RevertAid First Strand cDNA Synthesis kit (Fermentas GmbH, St. Leon-Rot, Germany). We prepared each sample with (+RT) and without (–RT) MuLV reverse transcriptase in parallel. This step was intended to detect contamination with genomic DNA later on.

SNP discovery

In order to identify SNPs in the transcribed regions of the candidate imprinted genes, genomic DNA from C57BL/6, Cast/Ei and F1 hybrid mice was subjected to PCR amplification (primer sequences and PCR conditions are available on request). By direct sequencing of the PCR products, we identified heterozygous tSNPs using an ABI 3730 DNA Analyzer and the BigDye Terminator v1.1 Cycle Sequencing kit (Applied Biosystems, Foster City, CA, USA).

Allelic expression analysis by QUASEP

The cDNA samples were amplified by PCR using one biotinylated primer per pair (primer sequences and PCR conditions are available on request). We next used the QUASEP approach for allelic expression analysis, as described previously (9). Owing to occasional background signals, depending on the particular assay, the peak heights must be normalized. Therefore, we repeated the QUASEP experiments at least four times for the homozygous B6 and Cast/Ei samples and 10 times for the heterozygous F1 hybrid and backcross samples and thereby calculated arithmetic mean and standard

deviation. With the results of the B6 and Cast/Ei samples, we drew calibration curves. We created these curves, representing the expected versus the measured relative amounts of a certain allele, for each QUASEP assay by linear regression analysis. Afterwards, we calculated the real allele ratio in F1 hybrid and backcross mice by interpolating the measured ratios by means of the calibration curve. For analysing the human *KCNK9* gene, we used genomic DNAs of different homozygous and heterozygous samples for comparing and normalizing the data obtained from RT-PCR products, as described earlier.

Programs used for sequence analysis

We used EMBOS CpGPlot in order to identify putative CpG islands (<http://www.ebi.ac.uk/emboss/cpgplot/>). The following parameters were used: GC content of $\geq 50\%$, observed/expected ratio of ≥ 0.6 and window of 100 bp with a length of ≥ 500 bp. For the identification of putative CTCF binding sites, we employed the CTCF finder tool that comprises all known CTCF sequence motifs (<http://www.essex.ac.uk/bs/molonc/spa.htm>).

Bisulphite sequencing

We performed bisulphite treatment using the EpiTect Bisulfite Kit (Qiagen) and PCR-amplified the converted DNA with primers specific for mCpG1, mCpG2, hCpG1 and hCpG2. In the case of mouse oocytes, treatments were performed on aliquots of approximately 150 oocytes and PCR amplifications were carried out on approximately 30 oocyte equivalents. We amplified two subregions from mCpG1 associated with the mouse *Kcnk9* promoter with the following primers: forward 5'-GTTAGAGTTTTAGGATTTT-3' and reverse 5'-TCTATCTAACAAAAACAAC-3' (subregion 1, T_{ann} 48.6°C, product size: 360 bp, with two SNPs between B6 and *M. spretus*) and forward 5'-GTTTGATTTAGGTTTGGTATA-3' and reverse 5'-CCACCTAAAACTAAAAAATC-3' (subregion 2, T_{ann} 53.9°C, product size: 493 bp, with two SNPs between B6 and *M. spretus*). For mCpG2 in the *Peg13*-DMR, two subregions were amplified with the following primer sets: forward 5'-TTTTGATTAATTGTGGGGTT-3' and reverse 5'-AAATAACTAACAAACCACC-3' (subregion 1, T_{ann} 53.5°C, product size: 298 bp) and forward 5'-AGGTTTTGTGTGATAGTTTA-3' and reverse 5'-CCTATCCACAAAATAAATAAC-3' (subregion 2, T_{ann} 53.5°C, product size: 366 bp). For hCpG1 associated with the human *KCNK9* promoter, we carried out PCR at 50°C with the following primers: forward 5'-TAGGGGATTTTAGAGATAT-3' and reverse 5'-ACAAACACAAAAACTACTC-3' (product size: 387 bp). For hCpG2 associated with the positionally conserved *Peg13*-DMR orthologous region in humans, we performed PCR at 57°C with the following primers: forward 5'-TTGAGATTTATTTGGGTGTTT-3' and reverse 5'-TCTCAATACATAACTTCAACATCC-3' (product size: 299 bp). We cloned the PCR products using the pGEM-T Vector Systems (Promega, Mannheim, Germany) and sequenced positive clones using the CEQ™ DTCS Quick Start Kit (Beckman Coulter, Krefeld, Germany) and a Beckman CEQ 8000 Genetic Analysis System. For bisulphite analysis performed at the Babraham Institute, pGEM-Teasy

clones were sequenced commercially (Cogenics Lark UK, Takeley, Essex). Sequences were analysed using the BiQ_Analyzer program (34). Sequences that could not be distinguished on the basis of identical patterns of non-converted cytosines were discarded as possible clonal in origin.

SUPPLEMENTARY MATERIAL

Supplementary Material is available at HMG Online.

ACKNOWLEDGEMENTS

We are thankful to Cornelia Wetzig for excellent technical assistance as well as Wendy Dean for assistance with mouse oocyte collection. Moreover, we thank Tim Tralau, Larissa Seidmann and Annette Müller for providing human tissue samples.

Conflict of Interest statement. None declared.

FUNDING

German Academic Exchange Service (DAAD) fellowship to N.R.; German Research Foundation (DFG) (HA 1374/8-1 and ZE 442/3-1 to T.H. and U.Z.); DFG to S.B. and F.C.L.; Biotechnology and Biological Sciences Research Council (BBSRC) to G.K.

REFERENCES

1. Reik, W. and Walter, J. (2001) Genomic imprinting: parental influence on the genome. *Nat. Rev. Genet.*, **2**, 21–32.
2. Li, E. (2002) Chromatin modification and epigenetic reprogramming in mammalian development. *Nat. Rev. Genet.*, **3**, 662–673.
3. Murphy, S.K. and Jirtle, R.L. (2003) Imprinting evolution and the price of silence. *Bioessays*, **25**, 577–588.
4. Morison, I.M., Ramsay, J.P. and Spencer, H.G. (2005) A census of mammalian imprinting. *Trends Genet.*, **21**, 457–465.
5. Peters, J. and Beechey, C. (2004) Identification and characterisation of imprinted genes in the mouse. *Brief Funct. Genomics Proteomics*, **2**, 320–333.
6. Smith, R.J., Arnaud, P. and Kelsey, G. (2004) Identification and properties of imprinted genes and their control elements. *Cytogenet. Genome Res.*, **105**, 335–345.
7. Luedi, P.P., Hartemink, A.J. and Jirtle, R.L. (2005) Genome-wide prediction of imprinted murine genes. *Genome Res.*, **15**, 875–884.
8. Nikaido, I., Saito, C., Mizuno, Y., Meguro, M., Bono, H., Kadomura, M., Kono, T., Morris, G.A., Lyons, P.A., Oshimura, M. *et al.* (2003) Discovery of imprinted transcripts in the mouse transcriptome using large-scale expression profiling. *Genome Res.*, **13**, 1402–1409.
9. Ruf, N., Dunzinger, U., Brinckmann, A., Haaf, T., Nurnberg, P. and Zechner, U. (2006) Expression profiling of uniparental mouse embryos is inefficient in identifying novel imprinted genes. *Genomics*, **87**, 509–519.
10. Bentley, L., Nakabayashi, K., Monk, D., Beechey, C., Peters, J., Birjandi, Z., Khayat, F.E., Patel, M., Preece, M.A., Stanier, P. *et al.* (2003) The imprinted region on human chromosome 7q32 extends to the carboxypeptidase A gene cluster: an imprinted candidate for Silver–Russell syndrome. *J. Med. Genet.*, **40**, 249–256.
11. Chapman, C.G., Meadows, H.J., Godden, R.J., Campbell, D.A., Duckworth, M., Kelsell, R.E., Murdock, P.R., Randall, A.D., Rennie, G.I. and Gloger, I.S. (2000) Cloning, localisation and functional expression of a novel human, cerebellum specific, two pore domain potassium channel. *Brain Res. Mol. Brain Res.*, **82**, 74–83.
12. Medhurst, A.D., Rennie, G., Chapman, C.G., Meadows, H., Duckworth, M.D., Kelsell, R.E., Gloger, I.I. and Pangalos, M.N. (2001) Distribution analysis of human two pore domain potassium channels in tissues of the

- central nervous system and periphery. *Brain Res. Mol. Brain Res.*, **86**, 101–114.
13. Yatsuki, H., Joh, K., Higashimoto, K., Soejima, H., Arai, Y., Wang, Y., Hatada, I., Obata, Y., Morisaki, H., Zhang, Z. *et al.* (2002) Domain regulation of imprinting cluster in Kip2/Lit1 subdomain on mouse chromosome 7F4/F5: large-scale DNA methylation analysis reveals that DMR-Lit1 is a putative imprinting control region. *Genome Res.*, **12**, 1860–1870.
 14. Ohlsson, R., Renkawitz, R. and Lobanenkov, V. (2001) CTCF is a uniquely versatile transcription regulator linked to epigenetics and disease. *Trends Genet.*, **17**, 520–527.
 15. Smith, R.J., Dean, W., Konfortova, G. and Kelsey, G. (2003) Identification of novel imprinted genes in a genome-wide screen for maternal methylation. *Genome Res.*, **13**, 558–569.
 16. Kim, D. (2005) Physiology and pharmacology of two-pore domain potassium channels. *Curr. Pharm. Des.*, **11**, 2717–2736.
 17. Zanzouri, M., Lauritzen, I., Duprat, F., Mazzuca, M., Lesage, F., Lazdunski, M. and Patel, A. (2006) Membrane potential-regulated transcription of the resting K⁺ conductance TASK-3 via the calcineurin pathway. *J. Biol. Chem.*, **281**, 28910–28918.
 18. Patel, A.J. and Lazdunski, M. (2004) The 2P-domain K⁺ channels: role in apoptosis and tumorigenesis. *Pflugers Arch.*, **448**, 261–273.
 19. Holter, J., Carter, D., Leresche, N., Crunelli, V. and Vincent, P. (2005) A TASK3 channel (KCNK9) mutation in a genetic model of absence epilepsy. *J. Mol. Neurosci.*, **25**, 37–51.
 20. Mu, D., Chen, L., Zhang, X., See, L.H., Koch, C.M., Yen, C., Tong, J.J., Spiegel, L., Nguyen, K.C., Servoss, A. *et al.* (2003) Genomic amplification and oncogenic properties of the KCNK9 potassium channel gene. *Cancer Cell*, **3**, 297–302.
 21. Kim, C.J., Cho, Y.G., Jeong, S.W., Kim, Y.S., Kim, S.Y., Nam, S.W., Lee, S.H., Yoo, N.J., Lee, J.Y. and Park, W.S. (2004) Altered expression of KCNK9 in colorectal cancers. *Apmis*, **112**, 588–594.
 22. Pei, L., Wiser, O., Slavin, A., Mu, D., Powers, S., Jan, L.Y. and Hoey, T. (2003) Oncogenic potential of TASK3 (Kcnk9) depends on K⁺ channel function. *Proc. Natl Acad. Sci. USA*, **100**, 7803–7807.
 23. Murrell, A. (2006) Genomic imprinting and cancer: from primordial germ cells to somatic cells. *Sci. World J.*, **6**, 1888–1910.
 24. Lin, S.P., Youngson, N., Takada, S., Seitz, H., Reik, W., Paulsen, M., Cavaille, J. and Ferguson-Smith, A.C. (2003) Asymmetric regulation of imprinting on the maternal and paternal chromosomes at the Dlk1-Gtl2 imprinted cluster on mouse chromosome 12. *Nat. Genet.*, **35**, 97–102.
 25. Thorvaldsen, J.L., Duran, K.L. and Bartolomei, M.S. (1998) Deletion of the H19 differentially methylated domain results in loss of imprinted expression of H19 and Igf2. *Genes Dev.*, **12**, 3693–3702.
 26. Youssef, E.M., Chen, X.Q., Higuchi, E., Kondo, Y., Garcia-Manero, G., Lotan, R. and Issa, J.P. (2004) Hypermethylation and silencing of the putative tumor suppressor Tazarotene-induced gene 1 in human cancers. *Cancer Res.*, **64**, 2411–2417.
 27. Cowles, C.R., Hirschhorn, J.N., Altshuler, D. and Lander, E.S. (2002) Detection of regulatory variation in mouse genes. *Nat. Genet.*, **32**, 432–437.
 28. Allen, E., Horvath, S., Tong, F., Kraft, P., Spiteri, E., Riggs, A.D. and Marahrens, Y. (2003) High concentrations of long interspersed nuclear element sequence distinguish monoallelically expressed genes. *Proc. Natl Acad. Sci. USA*, **100**, 9940–9945.
 29. Greally, J.M. (2002) Short interspersed transposable elements (SINEs) are excluded from imprinted regions in the human genome. *Proc. Natl Acad. Sci. USA*, **99**, 327–332.
 30. Ke, X., Thomas, N.S., Robinson, D.O. and Collins, A. (2002) The distinguishing sequence characteristics of mouse imprinted genes. *Mamm. Genome*, **13**, 639–645.
 31. Wang, Z., Fan, H., Yang, H.H., Hu, Y., Buetow, K.H. and Lee, M.P. (2004) Comparative sequence analysis of imprinted genes between human and mouse to reveal imprinting signatures. *Genomics*, **83**, 395–401.
 32. Bock, C., Paulsen, M., Tierling, S., Mikeska, T., Lengauer, T. and Walter, J. (2006) CpG island methylation in human lymphocytes is highly correlated with DNA sequence, repeats, and predicted DNA structure. *PLoS Genet.*, **2**, e26.
 33. Coombes, C., Arnaud, P., Gordon, E., Dean, W., Coar, E.A., Williamson, C.M., Feil, R., Peters, J. and Kelsey, G. (2003) Epigenetic properties and identification of an imprint mark in the Nesp-Gnasxl domain of the mouse Gnas imprinted locus. *Mol. Cell. Biol.*, **23**, 5475–5488.
 34. Bock, C., Reither, S., Mikeska, T., Paulsen, M., Walter, J. and Lengauer, T. (2005) BiQ analyzer: visualization and quality control for DNA methylation data from bisulfite sequencing. *Bioinformatics*, **21**, 4067–4068.